THE EFFECTS OF PYROLYSIS CONDITIONS ON THE MACROPORE STRUCTURE OF COAL CHARS

Kyriacos Zygourakis
Department of Chemical Engineering
Rice University
Houston, TX 77251-1892

INTRODUCTION

Pyrolysis is the first stage of direct coal utilization processes. As coal particles are heated in a reactor, they release most of their volatile constituents in the form of gases and tars. The chemical transformations characterizing the pyrolysis stage are accompanied by complex morphological transformations that determine the pore structure and, consequently, the reactivity of the produced chars during the subsequent combustion or gasification stage. Gasification processes are usually diffusion-limited since the various heterogeneous reactions take place at elevated temperatures. Low utilization of the surface area associated with the micropores present in chars is expected under such conditions. Reactions occur mostly in the larger macropores that are close to the particle exterior and pore accessibility to reactants becomes a major factor in determining gasification rates. Initially, internal pores may be inaccessible to reactants. As the reaction proceeds, however, walls of closed pores will burn away exposing surface area previously unavailable for reaction and leading to substantial particle fragmentation. The opening of closed porosity, the formation of a progressively more tortuous particle exterior and the fragmentation of the original particles can lead to large enhancements of the observed gasification rates.

The major factors affecting the macropore structure of chars are the rank of the parent coals and the pyrolysis conditions. Coals can be broadly categorized as **plastic** or **non-plastic** according to their behavior during pyrolysis. Plastic coals soften as they are heated up and behave as highly viscous non-newtonian fluids over a broad temperature range. Three phases are found to coexist during this plasticity stage: a viscous (but optically isotropic) coal melt, an anisotropic liquid crystalline phase and a gaseous phase. The volatile gases form bubbles that grow and coalesce swelling the coal particles and leading to the formation of highly cellular internal pore structures that are characteristic of chars derived from plastic coals. Non-plastic coals, on the other hand, do not soften and do not undergo drastic macropore structure transformations during the pyrolysis stage. Bituminous and subbituminous coals are generally considered to be plastic, while lignites and other low rank coals belong to the non-plastic category.

The operating conditions influencing most strongly the pyrolysis process are the heating rate, the particle size and the pressure. Existing literature data offer little quantitative information on the effect of operating conditions on macropore structures, since the majority of past studies have concentrated on studying the kinetics of pyrolysis reactions and the distributions of the obtained products. Previous studies (Howard, 1981; Oh et al., 1984), however, indicate that the kinetic and transport processes occurring during pyrolysis (such as the rate of volatile release, the diffusion of volatiles into the bubbles, the transport of volatiles to the particle exterior etc.) will be governed by the time-temperature history of the coal particles. Hence, the pyrolysis heating rate is expected to have the strongest effect on the macropore structure of the chars (Hamilton, 1981).

EFFECTS OF PYROLYSIS HEATING RATE ON MACROPORE STRUCTURE OF CHARS

A plastic coal (Illinois #6) was studied first. Coal particles in the 50-60 mesh (250-300 μm) range were pyrolyzed in a captive sample microreactor at five different heating rates: 0.1, 1.0, 10, 100 and 1000 °C/s. Char particles

collected from ten runs at each set of conditions were embedded in an epoxy-resin block, and one side of the block was polished to reveal random cross-sections. Digitized images for 50 particle sections were acquired from each block and they were analyzed with the digital image processor to obtain the size distribution of the two-dimensional macropore profiles. Fig. 1 presents binary images of representative cross-sections of char particles produced at the various heating rates. The black areas of these images correspond to the char matrix, while the internal white areas are the cross-sectional profiles of macropores.

The lowest heating rate (0.1 °C/s) produced char particles exhibiting a few scattered large cavities with thick walls and several smaller cavities. This is consistent with the accepted pyrolysis mechanism involving formation and growth of volatile gas bubbles. Note that most of the particles shown in Fig. 1A have retained their angular shape and only a few cenospheres were observed. Calculations indicated a moderate pressure buildup in the particle interior, since the volatile production rates are slow enough to let the gas escape before the bubbles can grow to a large size. At faster heating rates, however, the volatile production rates increase substantially leading to considerably higher pressures in the particle interior and, thus, to larger bubble sizes and more particle swelling. At a heating rate of 1 °C/s, the formation of several thin-walled cavities was observed (Fig. 1B) and several pyrolyzed char particles started exhibiting a distinct cellular internal structure. At still higher heating rates, the cellular internal structure was dominant. Chars pyrolyzed at 100 and 1000 °C/s showed exclusively thin-walled cellular structures with a few large cavities and a group of smaller secondary vesicles formed in the thin walls of the larger ones. One should note also that large particle swelling occurs at the higher heating rates leading to particles with very high porosity.

Table I summarizes the basic stereological properties for the five Illinois #6 chars. Estimates of the macroporosity ε can be obtained (Weibel, 1980) from the two-dimensional particle cross-sections using the formula $\varepsilon = A_a/A_c$, where A_a is the total area of pore profiles and A_c is the total area of the char particle sections. An estimator of the macropore surface density S_v (in (cm^2 pore surface)/(cm^3 particle)) is given (Weibel, 1980) by $S_a = B_a/A_c$, where B_a is the total pore profile boundary length and A_c is the total area of particle cross-sections. Both ε and S_v can be estimated from two-dimensional sections without any restricting assumptions concerning the geometrical shape of the pores (DeHoff, 1983). We have also obtained the macropore volume distributions, but these measurements were based on the assumption that the macropores can be modeled as non-overlapping spheres with randomly distributed radius.

Increasing heating rates produced chars with consistently higher porosity and maximum pore radius. The increase in porosity, however, tends to level off at the higher heating rates. An increase in the macropore surface area density S_v was observed as the pyrolysis heating rate increased from 0.1 to 10 °C/s. However, S_v decreased at higher heating rates due to the appearance of very large pore cavities in the highly-swollen char particles (see Figs. 1D and 1E). The property of interest for reaction engineering calculations, however, is the specific macropore surface area S_g expressed in (cm^2 pore surface)/(cm^3 solid char). Table I shows that S_g increased dramatically with increasing heating rates. This is an indication that Illinois #6 chars produced at high pyrolysis heating rates will be more reactive at elevated temperatures where low utilization of the micropores is expected.

Pyrolysis heating rates had a much smaller effect on the macropore structure of chars produced from a non-plastic lignite coal (Wilcox, Texas). Earlier indirect measurements have indicated that the initial macropore network of non-plastic (low rank) coals remains essentially intact during pyrolysis (Gavalas and Wilks, 1980). In order to study the effect of pyrolysis heating rate on the lignite char structure, coal particles in the the 50-60 mesh size range were pyrolyzed in our microreactor at three heating rates (0.1, 10 and 1000 °C/s). Fig. 2 shows

representative images of the polished char sections taken for each sample. In contrast to the Illinois#6 chars, the cross-sections of lignite char particles show almost no visible change as the heating rate is increased. A comparison of particle sections obtained from the pyrolyzed chars and the parent coal revealed that several large fractures and cracks were formed during the pyrolysis stage. Table II presents the basic structural properties for the lignite chars. These stereological measurements show small effects of the pyrolysis heating rate both on the particle porosity and on the specific macropore surface area S_g of the char samples.

EFFECTS OF COAL PARTICLE SIZE ON MACROPORE STRUCTURE OF CHARS

Heat transfer in pyrolyzing coal particles can be significantly affected by the particle size. If external heat transfer controls the pyrolysis process, particle temperature will remain constant during heatup and the heating rate will decrease with increasing particle size. On the other hand, if the rate of external heat transfer is high enough, high heating rates and large particle sizes can lead to significant temperature gradients within the particle. Under such conditions, the pyrolysis reaction rates will vary significantly inside the particles.

In order to quantify the effects of particle size on the macropore structure of chars produced from the Illinois #6 coal, two additional size fractions of coal particles were pyrolyzed at 10 °C/s: 25-28 mesh (589-710 μm particle diameter) and 100-120 mesh (125-149 μm particle diameter). Thus, the mass of individual particles varied by about two orders of magnitude for the pyrolysis runs at 10 °C/s. This heating rate was selected in order to facilitate the detection of differences in the pore structure possibly caused by changes in the internal heating rate of the particles.

Fig. 3 presents representative cross-sections of char particles produced from the additional runs at 10 °C/s. A comparison of the cross-sections shown in Fig. 3 and Fig. 1C reveals very different pore structures for the three chars. For the smallest size fraction (Fig. 3A), we observe fewer pores per particle and the pore shape is rather rounded. The largest size fraction, on the other hand, exhibits numerous macropores per particle. The boundaries of the pore profiles are very tortuous and we see again the characteristic cellular pore structure with small pores embedded in the walls separating the larger cavities.

Table III summarizes the measurements for the macropore properties. The interesting result here is that the macroporosity of the particles was not affected by their size. This indicates that particle size did not affect the internal heating rate, pointing out that external heat transfer is not limiting for our pyrolysis reactor. The maximum pore radius observed fell from 284 μm for the 25-28 mesh sample to 51 μm for the 100-120 mesh sample. This decrease in macropore size was accompanied by an increase in the specific surface area of macropores per unit volume of char particle.

It must be noted here that maceral segregation may complicate the determination of particle size effects on the macropore structure of chars produced from plastic coals. Due to differences in the mechanical properties of the various coal macerals, grinding and sifting procedures may lead to enrichment of certain macerals in certain size fractions (i.e. small size fractions may contain more exinite). Thus, the well-known differences in the plastic behavior and volatile content of coal macerals can affect the macropore structure of different size fractions.

MODELING OF CHAR GASIFICATION

Discrete models were developed to treat the problem of char gasification at high temperatures. Low utilization of the surface area associated with the micropores is expected under such conditions, and the accessibility and surface area of the

macropores become the dominant factors in determining the temporal evolution of reaction rates.

Our earlier discrete models (Sandmann and Zygourakis, 1986) defined the pores of a solid reactant (char) by overlapping regular geometrical entities (circles, spheres or cylinders) of a given size distribution. For example, two-dimensional simulations modeled the pore cross-sections as an assemblage of overlapping circles, grew the pores by increasing the circle diameters by a fixed amount at each time step and then determined which cells had to be changed (from char to pore) to reflect the new pore dimension. As shown in Figs. 1 through 5, however, highly irregular pore structures are observed when char particle cross-sections are viewed under the microscope.

The new discrete models are based on an **erosion algorithm** and they avoid the computational complexities introduced when pores of arbitrary geometry are approximated by overlapping regular geometric entities. These models again employ a computational grid to represent the reacting porous solid and the macropores. However, the initial computational grids are obtained directly from digitized images of actual particle cross-sections viewed under the microscope. These images are accurate discrete approximations of a slice of the actual reacting solid. The incorporation of sophisticated digital image processing techniques in the gasification models is perhaps the most attractive feature of the new approach. For the runs presented below, the following assumptions were made.

- Only the surface area directly accessible to reactants from the irregular particle exterior participates in the reaction. Macropores in the particle interior are not initially available for reaction. When the reaction front reaches these interior pores, however, their surface area becomes available for reaction.
- Diffusional limitations in the macropores that are open to the exterior are neglected. This assumption is not expected to lead to significant errors in model predictions for the Illinois #6 chars given the large size of their internal cavities.
- Internal pores for any cross-section do not become available for reaction due to burn-through occurring at planes above or below the studied one.

The last two assumptions have been relaxed in more recent versions of the erosion algorithm. At each simulation step, the computational grid is scanned and the surface area available for reaction is identified. A statistical method is then used to erode away a single layer of pixels corresponding to the char matrix from the exterior of the char particle (and from the exterior of all particle fragments). A 3x3 neighborhood around each char pixel is examined to determine whether or not it is on an edge boundary and should be reacted. The number of pixels reacting at each step is counted and the solid reactant conversion is calculated. This process can be repeated until a specified conversion has been achieved. Particle fragmentation can also be investigated with this model by identifying all the isolated char fragments.

Fig. 4 presents the temporal evolution of reaction rates for the four particle cross sections presented in Fig. 1A. The dimensionless rate R_e and time θ are defined as

$$R_e = \frac{1}{m_o}\frac{dm}{dt}\Delta\tau \qquad \theta = \frac{t}{\Delta\tau} = \frac{t\ R_s(c,T)}{\Delta x\ \rho_s}$$

where m_o is the mass of unreacted char, (dm/dt) is the rate of change of the reacting char mass, $R_s(c,T)$ is the intrinsic reaction rate per unit of surface area, ρ_s is the density of the solid, Δx is the pixel size of the image and $\Delta\tau$ is the time required to react a layer of solid with uniform thickness equal to 1 μm.

The erosion rate for the particle exhibiting the large cenosphere (ILL106 in Fig. 1A) decreases initially and then jumps to very high levels when the large internal cavity opens up for reaction. At this point, the cross-section fragments considerably and disappears soon thereafter. The ILL102 particle in Fig. 1A has several large cavities with thin walls separating them from the particle exterior. Thus, the erosion rates calculated for this cross-section jump to very high values as these cavities open up at fairly low conversions (less than 20%) The ILL105 cross-section of Fig. 1A, on the other hand, exhibits numerous smaller cavities that open up for reaction at different time levels giving rise to the characteristic jumps in the reaction rate observed in the experiments by Sundback et. al. (1984). In this case the reaction rates remain at relatively high levels for a large time interval. Finally, the more "solid" cross-section of Fig. 1A (ILL101) exhibits a steady decrease in erosion rate for a long period of time until the single large cavity opens up. A large jump in the erosion rate is observed at this point and the rate decreases slowly after achieving its maximum value. Another interesting observation from Fig. 4 concerns the wide range of particle burnout times predicted by the discrete simulations. These variations are clearly attributed to the large internal cavities and the different macroporosities of the individual particles.

Simulation results from runs on all particle sections can provide an indication of the expected average gasification behavior for a char sample. Fig. 5 presents the average reaction rate vs. time patterns for the three Illinois #6 chars produced by pyrolyzing coal particles of different sizes at 10 °C/s. Due to its small particle size and large external surface area, the 100-120 mesh sample exhibits a high initial rate, a sharp rate maximum and very short reaction times. As the particle size is increased, the reaction rates decrease and their burnout times increase significantly.

ACKNOWLEDGMENT

This work was partially supported by the Department of Energy under the contract DE-FG22-87PC79930.

REFERENCES

Gavalas, G.R. and Wilks, K.A., AIChE J., 26, 201 (1980).

Hamilton, L.H., Fuel, 60, 955 (1981).

DeHoff, R.T., J. Microscopy, 131, 259 (1983).

Howard, J.B., "Fundamentals of Coal Pyrolysis and Hydropyrolysis", in Chemistry of Coal Utilization, p. 665, Elliott, M.A., Ed., John Wiley (1981).

Oh, M., Peters, W.A. and Howard, J.B., Procs. 1983 International Conference on Coal Science, p. 483, International Energy Agency (1983).

Sandmann, C.W. and Zygourakis, K., Chem. Eng. Sci., 41, 733 (1986).

Sundback, C.A., Beer, J.M. and Sarofim, A.F., Procs. 20th International Symposium on Combustion, p. 1495, Ann Arbor, Michigan, August 12-17 (1984).

Weibel, E.R., "Stereological Methods", vol. 2, Academic Press (1980).

TABLE I

Macropore Structural Properties of Illinois #6 Chars Produced at Various Heating Rates

Heating Rate	Porosity	Surface Area Density (cm^2/cm^3 particle)	Specific Surface Area (cm^2/cm^3 solid)	Maximum Pore Radius (μm)
0.1	0.356	527	822	135
1.	0.526	759	1,599	173
10.	0.709	908	3,116	153
100.	0.795	700	3,409	194
1000.	0.873	695	5,470	224

TABLE II

Macropore Structural Properties of Lignite Chars Produced at Various Heating Rates

Heating Rate	Porosity	Surface Area Density (cm^2/cm^3 particle)	Specific Surface Area (cm^2/cm^3 solid)	Maximum Pore Radius (μm)
0.1	0.140	1,011	1,176	31.0
10.	0.153	1,107	1,307	25.5
1000.	0.195	1,369	1,700	25.6

TABLE III

Effects of Coal Particle Size on the Macropore Structural Properties of Illinois #6 Chars

Particle Size (mesh)	Porosity	Surface Area Density (cm^2/cm^3 particle)	Specific Surface Area (cm^2/cm^3 solid)	Maximum Pore Radius (μm)
100-120	0.689	1,898	6,106	50.5
50- 60	0.708	908	3,116	153
25- 28	0.688	729	2,339	351

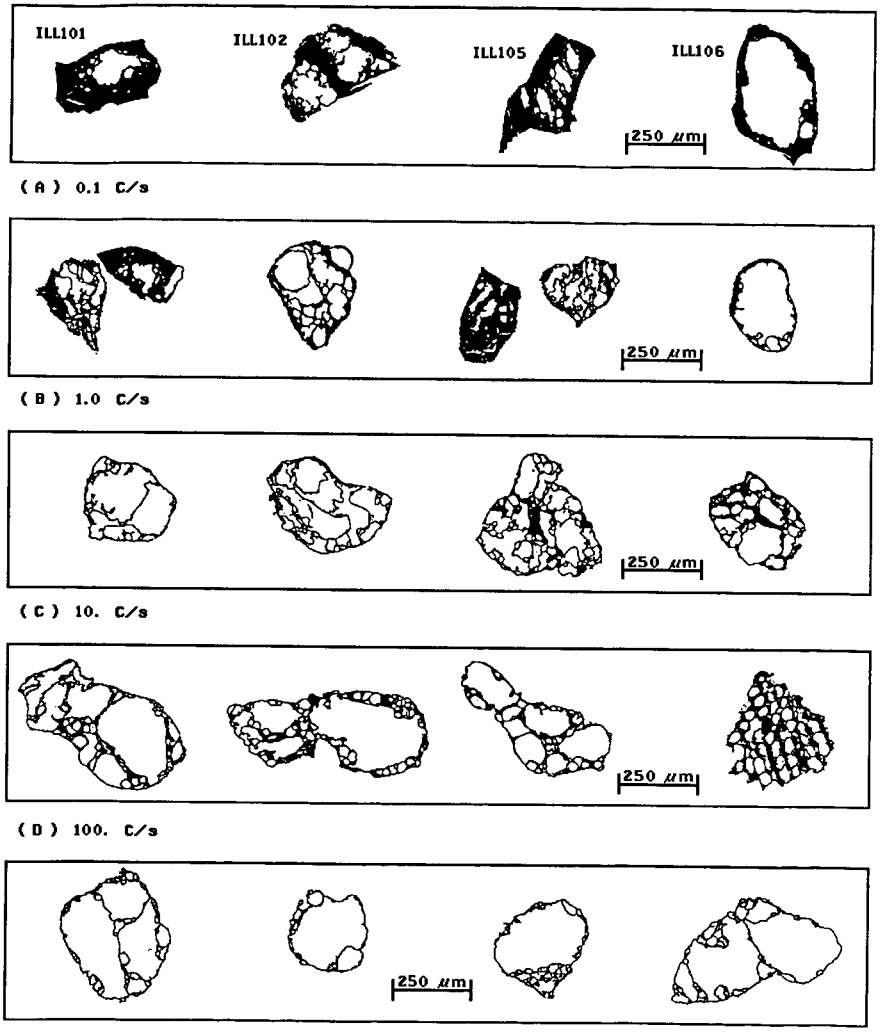

Figure 1: Binary images of particle cross-sections for Illinois #6 chars produced at various pyrolysis heating rates (Coal particle size: 50-60 mesh).

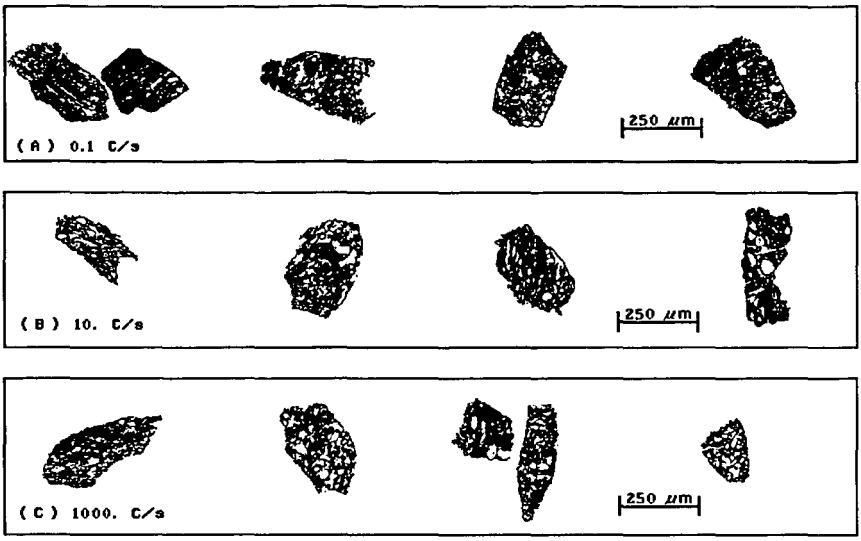

Figure 2: Binary images of particle cross-sections for lignite chars produced at various pyrolysis heating rates (Coal particle size: 50-60 mesh).

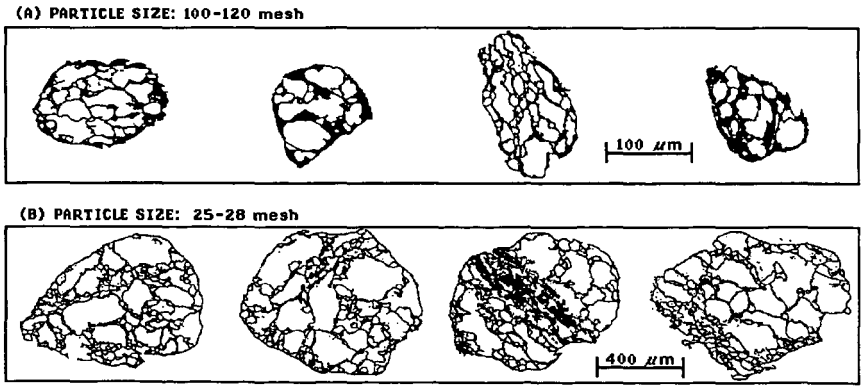

Figure 3: Binary images of particle cross-sections for Illinois #6 chars produced from different sizes of coal particles (Heating Rate: 10 °C/s).

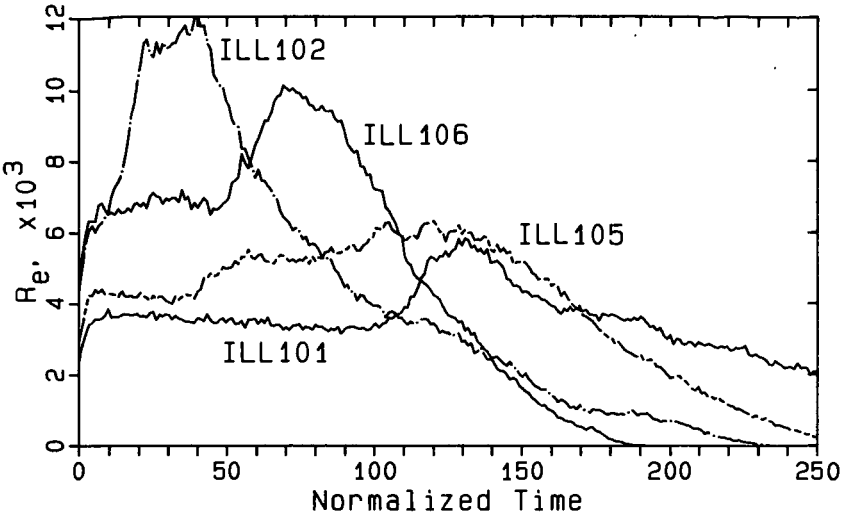

Figure 4: Temporal evolution of predicted reaction rates from four simulation runs with Illinois #6 char particles.

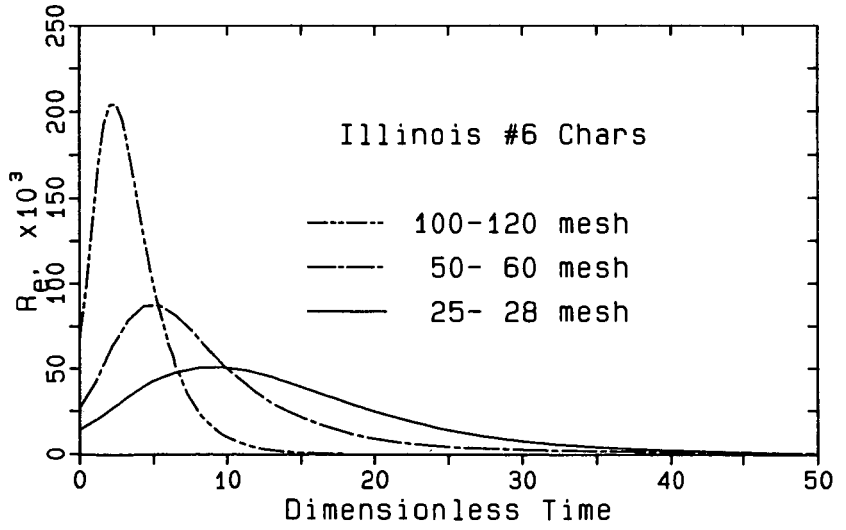

Figure 5: Effect of coal particle size on the reaction rates predicted for three Illinois #6 chars. Model predictions are averages for 48 particle cross-sections.